Key Engineering Materials
ISSN: 1662-9795, Vol. 840, pp 293-299
doi:10.4028/www.scientific.net/KEM.840.293
© 2020 Trans Tech Publications Ltd, Switzerland
Submitted: 2019-04-17
Revised: 2019-07-06
Accepted: 2019-11-11
Online: 2020-04-24

Synthesis of Nano-Hydroxyapatite from Snakehead (*Channa striata*) Fish Bone and its Antibacterial Properties

Poedji Loekitowati Hariani[1,a*], Muryati Muryati[2,b], Muhammad Said[1,c] and Salni Salni[3,d]

[1]Department of Chemistry, Faculty of Mathematics and Natural Sciences, Sriwijaya University, Jl. Palembang Prabumulih Km 32 Indralaya OI, Indonesia

[2]Master Programme in Department of Chemistry, Faculty of Mathematics and Natural Sciences, Sriwijaya University, Jl. Palembang Prabumulih Km 32 Indralaya OI, Indonesia

[3]Department of Biology, Faculty of Mathematics and Natural Sciences, Sriwijaya University, Jl. Palembang Prabumulih Km 32 Indralaya OI, Indonesia

[a]puji_lukitowati@mipa.unsri.ac.id, [b]muryatiengzlem@gmail.com, [c]msaidusman@unsri.ac.id, [d]salnibasir@unsri.ac.id

Keywords: Fish bone, synthesis, temperature, nano-hydroxyapatite, antibacterial

Abstract. Nano-hydroxyapatite was synthesized by coprecipitation method and tested its antibacterial properties. Nano-hydroxyapatite was synthesized using CaO precursors from snakehead (*Channa striata*) fish bones and $(NH_4)_2HPO_4$. The synthesis was carried out with temperature variations of 30, 60, 80, and 100 °C. Antibacterial activity was determined using two types of bacteria, namely gram-positive and gram-negative. The XRD spectra show that the highest peak is hydroxyapatite synthesized at a temperature of 100 °C. Hydroxyapatite produced from various synthesis temperatures has the size of nanoparticles in the range 37.32-49.27 nm. The nano-hydroxyapatite functional groups are characterized using FTIR, the analysis indicate the presence of OH, CO_3^{2-} and PO_4^{3-}. The molar ratio Ca/P is obtained of 1.71 approaching theoretical hydroxyapatite of 1.67. The resulted nano-hydroxyapatite has significant antibacterial properties to *Escherichia coli* and *Staphylococcus aureus.*

Introduction

Hydroxyapatite is the crystalline phase of the most stable calcium phosphate compound. The chemical formula of hydroxyapatite is $Ca_{10}(PO_4)_6(OH)_2$ [1]. Hydroxyapatite is commonly used in biomedical applications [2]. Many applications of hydroxyapatite include bone substitution, implant coating, composite implant components, dental material, and drug delivery [3]. The main component of enamel is hydroxyapatite which gives a white and bright color to the teeth [4]. In addition, the hydroxyapatite structure is similar to bone structure [5, 6]. Bone is complex body tissue which is composed of 65-70% hydroxyapatite, 20% collagen and water [7, 8]. Biomineralization studies show that the synthesized hydroxyapatite and its derivatives can be implanted in the human body as artificial bone [7, 9]. Hydroxyapatite is biocompatible and bioactive which can bind to bone tissue in the human body through osteoconductivity [6].

Hydroxyapatite contains large amounts of calcium and phosphate. Hydroxyapatite can be obtained from natural ingredients that contain lots of calcium, such as beef bone [10], salmon bones [6] robo labio bone [2], swordfish and tuna bones [11], eggshell [12], and arck clamshell [5]. The production of hydroxyapatite from fish bones has the advantage of being low cost and high purity [2]. Snakehead (*Channa striata*) fish is one type of fish that is widely consumed in Palembang, South Sumatra. Calcium content in the fish bone can be used as a precursor in hydroxyapatite synthesis. Other studies suggest that hydroxyapatite synthesized from *lates calcarifer* fish bone is noncytotoxic [13].

Hydroxyapatite can be synthesized using various methods such as heat treatment [2], wet ball milling [14], precipitation [15], and calcination [16]. One method that is often used is coprecipitation. This method is simple with a high success rate. In this study hydroxyapatite synthesis from snakehead fish bone by coprecipitation method was carried out. The process of calcination of fish bones produces

All rights reserved. No part of contents of this paper may be reproduced or transmitted in any form or by any means without the written permission of Trans Tech Publications Ltd, www.scientific.net. (#538846125, Sriwijaya University, Palembang, Indonesia-25/04/20,02:25:45)

CaO. After that, milling was carried out on CaO produced using ball milling to obtain nano-sized material. Nano-sized materials have different characteristics with bulk size. At a small size, it can improve the weakness of the mechanical properties of hydroxyapatite, and hydroxyapatite can fill a small hole on the enamel surface [4, 17].

In this work, the synthesis temperature is varied 30, 60, 80, and 100 °C. Synthesis temperature affects the crystallinity and particle size of the hydroxyapatite from the cockleshell [18]. Furthermore, the antibacterial activity was carried out using gram-positive bacteria and gram-negative bacteria. The bacteria used are *Staphylococcus aureus (S. aureus)* and *Escherichia coli (E. coli)*. The main problem with bone reconstruction is infection posted implant.

Experimental Section

CaO preparation. Fish bones were cut to pieces approximately 2-5 mm. 1 kg of fish bone boiled for 1 h, then washed and dried ±1 d. A total of 100 g of fish bone was soaked in 1 M HCl solution for 2 h, then washed until pH ±7 and dried at a temperature of 105 °C for 2 h in the oven. Dried fish bones were crushed and sifted 60 mesh. The fish bone powder was calcined at a temperature of 900 °C for 4 h in the furnace. Calcined CaO powder was smoothed using ball milling for 1 h with a weight ratio of CaO: the ball is 1:5.

Nano-hydroxyapatite synthesis. CaO powder (6 g) and 5 mL demineralized water were heated at a temperature of 30 °C for 30 min. 50 mL $(NH_4)_2HPO_4$ 1.66 M was added in the mixture. NH_4OH 1 M solution was added gradually until pH ±10 into the mixture while stirring using a magnetic stirrer and heated for ±2 h. After that, the solution was left for 24 h. The white-colored precipitate formed (nano-hydroxyapatite) was separated by filtering. The precipitate was dried using an oven at 105 °C for 2 h. The synthesis temperature was varied at temperatures of 30, 60, 80 and 100 °C. The hydroxyapatite synthesis reaction is as follows:

$$CaO + H_2O \rightarrow Ca(OH)_2$$

$$10Ca(OH)_2 + 6(NH_4)_2HPO_4 \rightarrow Ca_{10}(PO_4)_6(OH)_2 + 6H_2O + 12NH_4OH$$

Characterization. Hydroxyapatite products were observed for particle size and crystallinity using XRD Rigaku Miniflex 600. The nano-hydroxyapatite (nm) particle size can be determined using the following Scherrer equation:

$$d = \frac{0.9\,\lambda}{\beta\,\cos(\theta)} \quad (1)$$

Where d is particle size, λ is the wavelength of XRD radiation, θ is diffraction angle of diffraction peak, and β is full width at the half-maximum value of hydroxyapatite diffraction peak (211). Crystallization phase (X_c) is calculated using the following equation:

$$X_c = \frac{1 - \upsilon_{112/300}}{I_{300}} \quad (2)$$

Where I_{300} = intensity at peak (300) and $\upsilon_{112/300}$ = intensity at peak (112) and (300). The function group was determined using FTIR Thermo Scientific Nicolet iS10 at wavenumber 500-4000 cm^{-1}. Morphology and elements were determined using SEM-EDS JEOL JSM 6510-LA.

Antibacterial activity. Antibacterial activity tests were carried out using the diffusion method. The bacteria species of *E. coli* ATCC 25922 (gram-positive) and *S. aureus* ATTC 6358 (gram-negative) were obtained from PT Bio Farma. Variation in nano-hydroxyapatite concentrations was 12.5, 25, 50, 100, and 200 μg mL^{-1} using DMSO as a solvent. The test bacteria (0.1 mL) were each put into a petri dish containing 10 mL of nutrient agar. The mixture was homogenized by shaking until it freezes. After that, paper discs were placed on the surface of the media and pressed with a test solution (nano-hydroxyapatite) using a 10 μL micropipette. Petri dishes were wrapped in paper, for 24 h incubated at 37 °C in the incubator. The inhibitory diameter formed in millimeters was used to determine antibacterial activity.

Results and Discussion

Characterization of nano-hydroxyapatite. Fig. 1 shows the XRD pattern of nano-hydroxyapatite synthesized at temperatures 30, 60, 80, and 100 °C. The main diffraction peak of nano-hydroxyapatite at various temperatures following JCPDS No. 09-432. The nano-hydroxyapatite phase is characterized by the main intensity at a 2θ value 25.889°, 31.773°, 32.196°, 32.902°, 46.771°, and 49.468° which correlate with the field of hkl i.e. (002), (211), (112), (300), (222), and (213). The temperature of synthesis affects the intensity of the peak. It can be seen that the increase of synthesis temperature, the high the peak intensity. The highest peak is hydroxyapatite which is synthesized at 100 °C. Other research reported that hydroxyapatite synthesized in temperature 25 °C has an amorphous peak [19]. The heating process of fish bones releases collagen and proteins that are bound to fish bones.

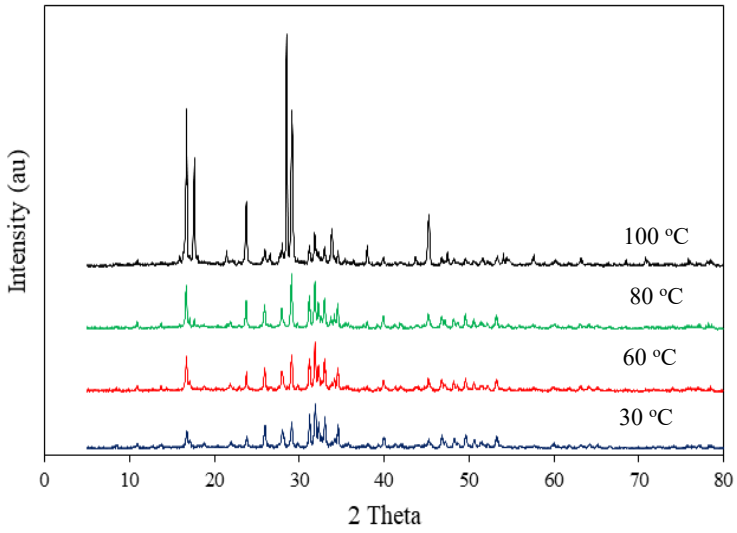

Figure 1. XRD spectra of nano-hydroxyapatite

Peak intensity affect on particle size and crystallinity. Table 1 show particle size and crystallinity increased with increasing synthesis temperature. Diffractogram of hydroxyapatite with sharp and narrow peaks shows that the compounds formed have high crystallinity [20]. Hydroxyapatite particle sizes at all synthesis temperatures are in nanoscale size (<100 nm), so it is classified as nano-hydroxyapatite. This particle size is greater than the hydroxyapatite from seashell with the same method, namely 101 nm [21]. The biggest crystallinity is obtained at 100 °C.

Table 1. Particle size and crystallization nano-hydroxyapatite at various synthesis temperatures

Temperature (°C)	The crystallite size (nm)	Crystallinity (%)
30	37.32	73.8
60	44.19	78.8
80	45.99	80.2
100	49.27	89.3

Fig. 2 shows the nano-hydroxyapatite FTIR spectra at wavenumbers 500-4000 cm^{-1}. The characteristic feature of the phosphate group can be observed in wavenumbers 500-1100 cm^{-1} [20]. The wavenumbers at 551-559 cm^{-1} and 597-599 cm^{-1} indicate the P–O group bending absorption. The wavenumber at 960-984 and 1050-1060 cm^{-1} correlated with stretching vibration of C–O bond. The OH stretching group appears at wavenumbers 3000-3500 cm^{-1} [22]. The carbonate group (CO_3^{2-}) derived from fish bone is still detected at wavenumbers 1400-1450 cm^{-1} where the peak intensity decreases as synthesis temperature increase. Natural bones contain carbonates in the amount

of 4-8% which are substituted by several elements such as Na^+, K^+, Mg^{2+}, F^-, Cl^-, etc [23]. The presence of CO_3^{2-} is also thought from reaction CO_2 in the atmosphere with precursors and substituting PO_4^{3-} [24].

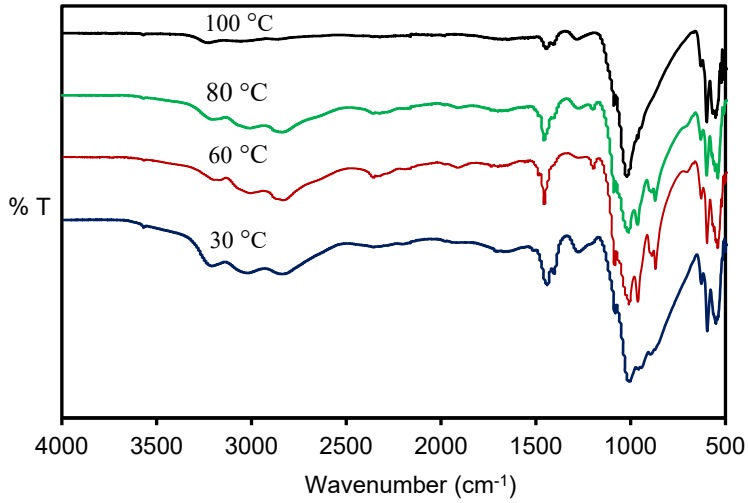

Figure 2. FTIR spectra of nano-hydroxyapatite

The morphology and element of nano-hydroxyapatite were analyzed using SEM-EDS. In this study, the analysis was carried out on nano-hydroxyapatite synthesized at a temperature of 100 °C. Morphology with a magnification of 40,000 times and spectra of EDS nano-hydroxyapatite can be seen in Fig. 3. The surface of nano-hydroxyapatite appears solid and shows the presence of pores in several locations.

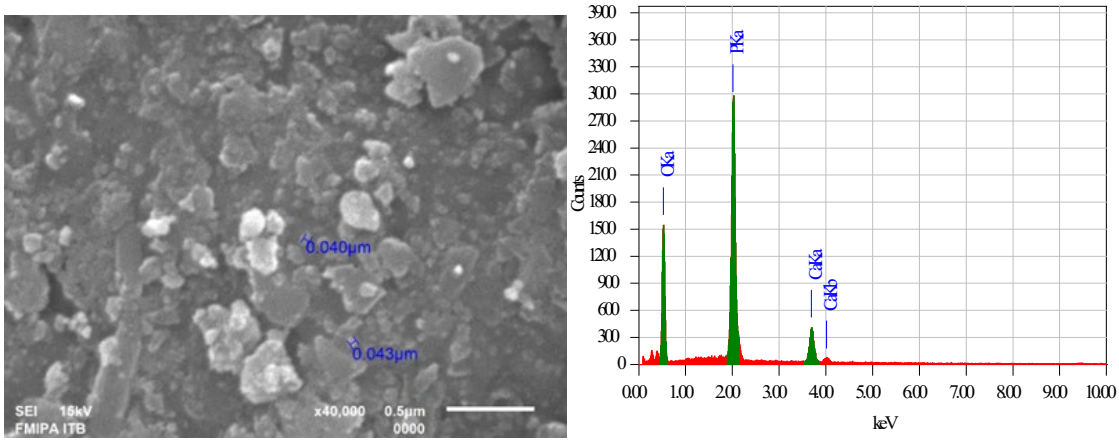

Figure 3. SEM micrograph and EDS spectra of nano-hydroxyapatite

The content of the nano-hydroxyapatite element is presented in Table 2. The molar ratio of Ca/P for theoretical nano-hydroxyapatite is 1.67 [25]. From EDS data can be calculated the molar ratio of Ca/P hydroxyapatite. The value of the molar ratio obtained is 1.71. A larger molar ratio indicates that some Ca did not react with the phosphate groups because they were still bound to the carbonates. The presence of carbonate ions appears in FTIR spectra. The carbonate group is often found in natural nano-hydroxyapatite [22].

The antibacterial effects of nano-hydroxyapatite have been extensively studied with various methods and types of bacteria [26]. These antibacterial properties are important in biomedical applications. Nano-hydroxyapatite has antibacterial ability better than its bulk size [4]. FTIR spectra indicated that hydroxyapatite contains carbonate. The presence of carbonate can increase hydroxyapatite bioactivity. Incorporation of hydroxyapatite with carbonates increases solubility, increasing the concentration of Ca and phosphate ions are important in bone formation [27].

Inhibitory diameter after the addition of nano-hydroxyapatite in *S. aureus* and *E. coli* bacteria shown in Fig. 4. The size of the inhibition zone is influenced by the type of test bacteria, size, and concentration of nanoparticles [28]. The higher concentration of antibacterial compounds used, the higher antibacterial activity produced [29]. The largest inhibition diameter at concentrations of 200 μg mL^{-1} ie 14.1 and 10.2 mm for *S. aureus* and *E. coli*.

Table 2. The elements of nano-hydroxyapatite

Elements	Mass (%)
O	53.07
Ca	32.29
P	14.64

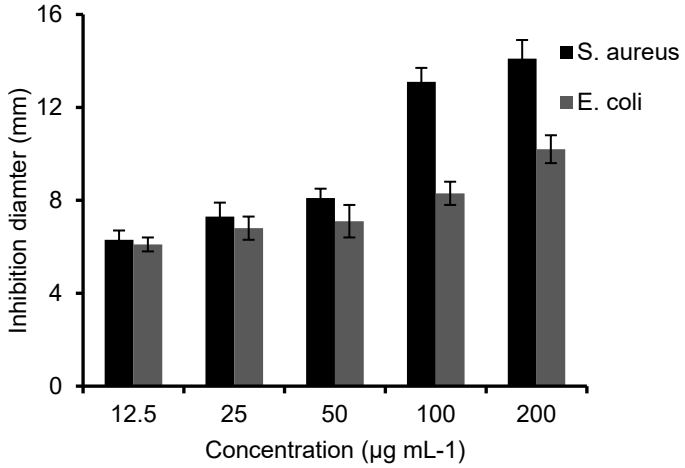

Figure 4. Antibacterial activity of nano-hydroxyapatite to *S. aureus* and *E. coli*

The mechanism inhibition can occur through several mechanisms namely, the OH group on nano-hydroxyapatite destroys the cell wall and the structure of bacterial proteins. In this study, the increase of temperature synthesis, the water evaporates so the OH group decreases but hydroxyapatite has greater crystallinity and purity which is suitable for bone implants. The OH group destroys bacterial cell walls by combining N-acetyl muramic acid into mucopeptide structures while the destruction of bacterial protein structures is caused by the occurrence of protein denaturation due to chemicals. Other literature states that inhibition is related to bacterial cell walls through the mechanism of peptidoglycan destruction. Hydrogen bonds between H atoms in hydroxyapatite and O atoms in peptidoglycan interfere with tetra-peptide bonds so that the bonds in peptidoglycan become unstable, and therefore peptidoglycan is easily destroyed [30]. The difference in diameter inhibition of the two bacteria is different due to differences in the membrane structure of the bacterial [31]. Gram-positive bacteria are bacteria that have a cell wall consisting of the main component of peptidoglycan which are permeable which usually does not limit the penetration of antimicrobial [32].

Summary

Nano-hydroxyapatite has been successfully synthesized from snakehead fish bone at various synthesis temperatures (30, 60, 80, and 100 °C) by coprecipitation method. The highest crystallinity was obtained from the synthesized nano-hydroxyapatite at the temperature of 100 °C with the crystallinity of 89.3% and particle size of 49.27 nm. Nano-hydroxyapatite has antibacterial properties in both test bacteria, gram-positive and gram-negative bacteria. Thus, nano-hydroxyapatite has the potential to be applied in biomedical.

Acknowledgement

This research is funded from the Kemenristek DIKTI, Indonesia by Hibah Penelitian Dasar Unggulan Perguruan Tinggi 2019.

References

[1] D. Ghahremani, I. Mobasherpour, E. Salahi, M. Ebrahimi, S. Manfi, L. Karamatpour, Potential of nano crystalline calcium hydroxyapatite for tin(II) removal from aqueous solution: equilibria and kinetic processes, Arabian J. Chem. 10 (2017) 461-471.

[2] B.R. Sunil, M. Jagannatham, Production hydroxyapatite from fish bone by heat treatment, Mater. Lett. 185 (2016) 411-414.

[3] J. Kolmas, E. Groszyk, D.K. Rozycka, Substituted hydroxyapatite with antibacterial properties, Biomed. Res. Int. 2014 (2014) 1-15.

[4] E. Pepla, L.K. Besherat, G. Palaia, G. Tenore, G. Migliau, Nano-hydroxyapatite and its applications in preventive, restorative, and regenerative dentistry: a review literature, Ann. Stomatol. 5 (2014) 108-114.

[5] M.Z.A. Khiri, K.A. Matori, N. Zainuddin, C.A.C. Abdullah, Z.N. Alassan, N.F. Baharuddin, M.H.M. Zaid, The usability of ark clam shell (*Anadara granosa*) as calcium precursor to produce hydroxyapatite nanoparticle via wet chemical precipitate method in various sintering temperature, SpringerPlus 5 (2016) 1-15.

[6] J. Venkatesan, B. Lowe, P. Manivasagan, K.H. Kang, E.P. Chalisserry, S. Anil, D.G. Kim, S.K. Kim, Isolation and characterization of nano-hydroxyapatite from salmon fish bone, Materials 8 (2015) 5426-5439.

[7] M.S. Shojai, M.T. Khorasani, E.D. Khoshdargi, A. Jamshidi, Synthesis methods for nanosized hydroxyapatite with diverse structures, Acta Biomater. 9 (2013) 7591-7621.

[8] A. Szcześ, L. Hołysz, E. Chibowski, Synthesis of hydroxyapatite for biomedical applications, Adv. Colloid Interface. Sci. 249 (2017) 321-330.

[9] X. Zhang, Preparation and Characterization of Calcium Phosphate Ceramics and Composites as Bone Substitutes, Dissertation, University of California United State, 2007.

[10] W. Khoo, F.M. Nor, H. Ardhyananta, D. Kurniawan, Preparation of natural hydroxyapatite from bovine femur bones using calcination at various temperatures, Procedia Manuf. 2 (2015) 196-201.

[11] M. Boutinguiza, J. Pou, R. Comesana, F. Lusquinos, A. De Carlos, B. Leon, Biological hydroxyapatite obtained from fish bone, Mater. Sci. Eng. C 32 (2012) 478-486.

[12] S.C. Wu, H.C. Hsu, S.K. Hsu, Y.C. Chang, W.F. Ho, Synthesis of hydroxyapatite from eggshell powder through ball milling and heat treatment, J. Asian Ceram. Soc. 4 (2016) 85-90.

[13] A. Pal, S. Paul, A.R. Choudhury, V.K. Balla, M. Das, A. Sinha, Synthesis of hydroxyapatite from lates calcalifer fish bone for biomedical applications, Mater. Lett. 203 (2017) 89-92.

[14] J. Zhang, T. Yin, S. Xiong, Y. Li, U. Ikram, R. Liu, Thermal treatments affect breakage kinetics and calcium release of fish bone particles during high-energy wet ball milling, J. Food Eng. 183 (2016) 74-80.

[15] N. Jamarun, S. Elfina, S. Arief, A. Djamaan, Mufitra, Hydroxyapatite material: synthesis by using precipitation method from limestone, Der Pharma Chem. 8 (2016) 302-306.

[16] T. Goto, K. Sasaki, Effects of trace elements in fish bones on crystal characteristics of hydroxyapatite obtained by calcination, Ceram. Int. 40 (2014) 10777-10785.

[17] M. Okada, T. Matsumoto, Synthesis and modification of apatite nanoparticles for use in dental and medical applications, Jpn. Dent. Sci. Rev. 51 (2015) 85-95.

[18] Y. Azis, Zultiniar, N. Jamarun, A. Syukrie, H. Nur, Hydrothermal synthesis of hydroxyapatite from cockle shell waste, Proceeding of Ocean, Mechanical and Aerospace -Science and Engineering in the 1st Conference on Ocean, Mechanical and Aerospace Scientists and Engineer, Pekan Baru, Indonesia, ISOMAse, 19-20 November 2014, pp. 167-170

[19] G. Wang, D. Zhao, Y. Ma, Z. Zhang, H. Che, J. Mu, X. Zhang, Z. Zhang, Synthesis and characterization of polymer-coated manganese ferrite nanoparticles as controlled drug delivery, Appl. Surf. Sci. 428 (2018) 258-263.

[20] D.J. Indrani, B. Soegijono, W.A. Adi, N. Trout, Phase composition and crystallinity of hydroxyapatite with various heat treatment temperatures, Int. J. App. Pharm. 9 (2017) 87-91.

[21] S. Santhosh, S.B. Prabu, Synthesis and characterization of nanocrystalline hydroxyapatite from sea shells, Int. J. Biomed. Nanosci. Nanotechnol. 2 (2012) 276-282.

[22] N.A.M. Barakat, M.S. Khil, A.M. Omran, F.A. Sheikh, H.Y. Kim, Extraction of pure natural hydroxyapatite from the bovine bones bio waste by three different methods, J. Mater. Process. Technol. 209 (2009) 3408-3415.

[23] L.T. Bang, B.D. Long, R. Othman, Carbonate hydroxyapatite and silicon-substituted carbonate hydroxyapatite: synthesis, mechanical properties, and solubility evaluations, Sci. World J. 2014 (2014) 1-9.

[24] P. Kamalanathan, S. Ramesh, L.T. Bang, A. Niakan, C.Y. Tan, J. Purbolaksono, H. Chandran, W.D. Teng, Synthesis and sintering of hydroxyapatite derived from eggshells as a calcium precursor, Ceram. Int. 40 (2014) 16349-16359.

[25] W. Pon-On, P. Suntornsaratoon, N. Charoenphandhu, J. Thongbunchoo, N. Krishnamra, I.M. Tang, Hydroxyapatite from fish scale for potential use as bone scaffold or regenerative material, Mater. Sci. Eng. C 62 (2016) 183-189.

[26] S.V. Raj, M. Rajkumar, N.M. Sundaram, A. Kandaswamy, Synthesis and characterization of hydroxyapatite/alumina ceramic nanocomposites for biomedical applications, Bull. Mater. Sci. 41 (2018) 1-8.

[27] G.S. Kumar, E.K. Girija, Flower like hydroxyapatite nanostructures obtained from eggshell: a candidate for biomedical applications, Ceram. Int. 39 (2013) 8293-8299.

[28] P.L. Hariani, Desnelli, Fatma, I.P. Rizki, Salni, Synthesis and characterization of Fe_3O_4 nanoparticles modified with polyethylene glycol as antibacterial material, J. Pure App. Res. 7 (2018) 122-129.

[29] G.S. Kumar, S. Rajendran, S. Karthi, R. Govindan, E.K. Girija, G. Karunakaran, D. Kuznetsov, Green synthesis and antibacterial activity of hydroxyapatite nanorods for orthopedic applications, MRS Commun. 7 (2017) 183-188.

[30] A. Safitri, A. Srihardyastutie, A. Roosdiana, S. Sutrisno, Antibacterial activity and phytochemical analysis of edible seaweed eucheuma spinosum against staphylococcus aureus, J. Pure App. Res. 7 (2018) 308-315.

[31] H.S. Ragab, F.A. Ibrahim, F. Abdallah, A.A. Al-Ghamdi, F. El-Tantawy, N. Radwan, F. Yakuphanoglu, Synthesis and in vitro antibacterial properties of hydroxyapatite nanoparticles, IOSR-Journal of Pharmacy and Biological Sciences 9 (2014) 77-85.

[32] M. Simões, S. Rocha, M.A. Coimbra, M.J. Vieira, Enhancement of escherichia coli and staphylococcus aureus antibiotic susceptibility using sesquiterpenoids, Med. Chem. 4 (2008) 616-623.